The Anatomy of Flagellar Microtubules: Polarity, Seam, Junctions, and Lattice

Young-Hwa Song and Eckhard Mandelkow

Max-Planck Unit for Structural Molecular Biology, Notkestraße 85, D-22603 Hamburg, Federal Republic of Germany

Abstract. Although the overall structures of flagellar and cytoplasmic microtubules are understood, many details have remained a matter of debate. In particular, studies of the arrangement of tubulin subunits have been hampered by the low contrast of the tubulin subunits. This problem can now be addressed by the kinesin decoration technique. We have shown previously that the recombinant kinesin head domain binds to β-tubulin, thus enhancing the contrast between α- and β-tubulin in the electron microscope; this allows one to study the arrangement of tubulin dimers. Here we describe the lattices of the four different types of microtubules in eukaryotic flagellar axonemes (outer doublet A and B, central pair C1 and C2). They could all be labeled with kinesin head with an 8-nm axial periodicity (the tubulin dimer repeat), and all of them showed the B-surface lattice. This lattice is characterized by a 0.92-nm stagger between adjacent protofilaments. The B-lattice was observed on the axonemal microtubules as well as on extensions made by polymerizing porcine brain tubulin onto axonemal microtubules in the proximal and distal directions. This emphasizes that axonemal microtubules serve as high fidelity templates for seeding microtubules.

The presence of a B-lattice implies that there must be a helical discontinuity ("seam") in the wall. This discontinuity is now placed near protofilaments A1 and A2 of the A-tubule, close to the inner junction between A- and B-microtubules. The two junctions differ in structure: the protofilaments of the inner junction (A1-B10) are staggered roughly by half a dimer, those of the outer junction (A10-B1) are roughly in register. Of the two junctions the inner one appears to have the stronger bonds, whereas the outer one is more labile and opens up easily, generating "composite sheets" with chevron patterns from which the polarity can be deduced (*arrow* in the plus direction).

Decorated microtubules have a clear polarity. We find that all flagellar microtubules have the same polarities. The orientation of the dimers is such that the plus end terminates with a crown of α subunits, the minus end terminates with β subunits which thus could be in contact with γ-tubulin at the nucleation centers.

INTRACELLULAR transport of vesicles and organelles requires motor proteins such as kinesin or dynein which move along tracks of microtubules; a well-known example is the anterograde transport in nerve axons powered by kinesin (Vale et al., 1985; Brady, 1985). This is a tetramer of two heavy and two light chains; the heavy chain consists of an NH_2-terminal motor domain (the head) responsible for microtubule binding and ATP hydrolysis, a stalk domain, and a COOH-terminal tail that is probably involved in light chain and vesicle attachment (Scholey et al., 1989; Yang et al., 1989; Kuznetsov et al., 1989; for reviews see Goldstein, 1991; Bloom, 1992; Walker and Sheetz, 1993). In our previous study (Song and Mandelkow, 1993), we have determined some structural properties of the mirotubule-kinesin complex. This was based on recombinant kinesin motor domain (derived from a squid kinesin cDNA clone, Kosik et al., 1990) and its interactions with taxol-stabilized porcine brain microtubules. The stoichiometry of binding was one kinesin head per tubulin dimer, chemical cross-linking showed preferential association with β-tubulin, and the periodicity of bound kinesin head along microtubules was 8 nm; a similar stoichiometry was observed by Harrison et al. (1993).

One of the unexpected features was that we could make use of the decoration of microtubules by kinesin to address the question of microtubule structure in a new way. This was possible because the bound kinesin head strongly enhances the contrast between α- and β-tubulin which otherwise is exceedingly weak. This allowed us to take a fresh look at the microtubule surface lattice. Two models had been proposed in the past, named A-lattice and B-lattice after the flagellar A- and B-microtubules where they were thought to occur (Figs. 1 and 2; Amos and Klug, 1974). Since only the A-lattice allowed helical symmetry, it was generally accepted that cytoplasmic microtubules should also have the A-lattice, even though a number of studies pointed to the B-lattice (Mandelkow et al., 1977, 1986; Crepeau et al., 1978; McEwen

Please address all correspondence to Dr. Eckhard Mandelkow, Max-Planck Unit for Structural Molecular Biology, Notkestraße 85, D-22603 Hamburg, FRG. Tel.: (49) 40 8998 2810. Fax: (49) 40 891314.

and Edelstein, 1980; Linck et al., 1981; Linck and Langevin, 1981). These earlier studies were limited by the lack of contrast between α and β which made clear cut conclusions difficult.

Knowing the microtubule lattice is important if one wants to understand a motile machinery such as the eukaryotic flagellum since all the components (dynein motors, spokes, nexins, etc.) are attached to the 9+2 microtubules and control their interplay in flagellar beating (for reviews see Murray 1991; Witman, 1992). We have therefore made a systematic study of the four types of microtubules occurring in flagellar axonemes, namely the A- and B-microtubules (which make up the outer doublets), and the two C-microtubules C1 and C2 which occur as singlets in the center of the flagellum. Here we show that all of them possess the B-lattice, implying that complete microtubules must have a seam which is probably located near the inner junction of the A-B tubules. We also found direct evidence that all flagellar microtubules have identical polarities, confirming the data of Euteneuer and McIntosh (1981) obtained by the hook assembly technique. Finally, we find that the plus ends have a crown of α subunits, and minus ends have a crown of β subunits, in agreement with the model of Oakley (1992). Since β-tubulin with bound GTP is near the plus end (Mitchison, 1993), this means that GTP becomes buried inside a protofilament as soon as tubulin assembly takes place.

Materials and Methods

Methods used in this study were mostly described previously (Song and Mandelkow, 1993) and are mentioned only briefly: phosphocellulose-purified brain tubulin was prepared from porcine brains (reassembly buffer 0.1 M Pipes pH 6.9, 1 mM $MgCl_2$, 1 mM EGTA, 1 mM DTT, and 1 mM GTP). Negative stain (2% uranyl acetate) electron microscopy was done on a Philips CM12 microscope. Optical diffraction was done on a diffractometer equipped with a HeNe laser and an f=100-cm lens.

Preparation of Axonemes, Outer Doublet Microtubules, and Central Pair Microtubules

Sperm flagellar axonemes were purified from sea urchin (*Psammechinus miliaris*) according to Gibbons and Fronk (1979). The sperm pellet was resuspended in 40 vol of a buffer (5 mM Tris-phosphate, pH 7.6, 0.5% NP-40, 1 mM EDTA, 2 mM $MgSO_4$, 1 mM ATP). The suspension was centrifuged at 3,000 g. The pellet was discarded and the supernatant was centrifuged at 12,000 g. The axoneme pellet (9+2 structure) was resuspended in reassembly buffer plus 50% glycerol and stored at −20°C. The outer doublet microtubules were isolated essentially using the method of Bell et al. (1982) by washing the axonemes repeatedly with high salt buffer (5 mM Imidazole pH 7.0, 600 mM NaCl, 4 mM $MgSO_4$, 1 mM $CaCl_2$, 1 mM EDTA, 1 mM DTT). For the experiments, the isolated outer doublet microtubules were dissolved in reassembly buffer. For the studies of central pairs, the axonemes were digested briefly (≈2 min) with trypsin (molar ratio trypsin to axonemal proteins ≈1:2,000). The digestion was stopped by addition of 2 mM PMSF. Trypsin was removed by pelleting of axonemes and changing the buffer twice (including 1 mM PMSF). The axonemes were then used for decoration with recombinant kinesin head.

Expression and Purification of Recombinant Kinesin Head Protein (43 kD)

The recombinant kinesin head protein was isolated essentially as described in Song and Mandelkow (1993). Briefly, *E. coli* HMS174(DE3) cells transformed with an expression vector for kinesin head (395 NH_2-terminal residues of squid kinesin heavy chain) were harvested 2 h after induction with 0.1 M isopropyl-β-D-thiogalacto-pyranoside (IPTG) and lysed with a French Press. Affinity purification of the high speed supernatant (100,000 g) was done with taxol-stabilized porcine brain microtubules in the presence of 1 mM adenosine 5'-(β,γ-imino) triphosphate (AMP-PNP). After incubation for 10 min at 25°C and pelleting for 20 min at 100,000 g, the kinesin head was redissociated from the microtubules with 10 mM MgATP. Further purification was done by MonoQ chromatography (gradient: 0.15–1.0 M KCl).

Analysis of Microtubule Lattice

The original description was given by Amos and Klug (1974), for a recent summary see Song and Mandelkow (1993). Briefly, the arrangement of tubulin monomers (disregarding the difference between α and β) in a microtubule can be described by several families of helices, including a shallow left-handed 3-start helix (inclination ≈10°, index: −3) or a steeper right-handed 10-start helix (inclination ≈30°, Fig. 2 *a*). These helices generate prominent diffraction peaks on the 4-nm layer line (since the axial repeat of monomers is 4 nm). Tubulin heterodimers (α-β) could in principle be aligned either parallel to the 10-start helix ("A"-lattice, originally proposed for A-tubules of flagellar outer doublets, Fig. 2 *a*) or along the 3-start helix ("B"-lattice, proposed for B-tubules, Fig. 2 *b*). The diffraction arising from the dimer helices would therefore point in the same direction as the corresponding monomer helices, except that the peaks would lie on an 8-nm layer line (since the dimer repeat is 8 nm, Fig. 2, *c* and *d*). For normal microtubules, the 8-nm layer line is virtually absent because the contrast between α- and β-tubulin is very weak (as if the shading were absent in Fig. 2, *a* and *b*). Additional reflections are expected on each layer line because of the multiplicity of helical families, superposition of front and back of a microtubule, and spurious effects due to flattening on the EM grid, uneven staining, and so forth, but this does not change the basic argument. The analysis becomes more clear cut and obvious when the microtubule opens up into a flat sheet (Erickson, 1974): extended reflections become sharp spots with higher contrast, and the pattern becomes simply one-sided (corresponding either to the front or back of a microtubule; examples see below).

Lattice Symmetry and Nomenclature

The fact that microtubules consist of tubulin dimers, have mostly 13 protofilaments, and a 3-start helix imposes constraints on the symmetry. The A-lattice could in principle be helically symmetric, but the B-lattice cannot; there has to be at least one discontinuity where the sequence of like subunits is interrupted by a junction between unlike subunits (Fig. 2 *b*). Thus the observation of a B-lattice implies the existence of one A-type interaction. We will refer to this arrangement as B-lattice since the B-type interaction is the predominant one. By contrast, a mixed lattice is one where A-type and B-type interactions are mixed in a random fashion (not observed so far, for review see Wade and Chretien, 1993).

Conventions and Terminology

A flagellar outer doublet contains one complete microtubule (A, 13 protofilaments) and one incomplete microtubule (B, usually 10, sometimes 11 protofilaments); our numbering of protofilaments follows that of Linck et al. (1981) (see Fig. 1). There are two "junctions" between these tubules, the inner junction (formed by protofilaments A1 and B10) and the outer junction (A10 and B1). The "common wall" between A and B tubules is formed by protofilaments A10, A11, A12, A13, and A1 (counting clockwise). The seam refers to the helical discontinuity which must exist in a complete microtubule with a B-lattice. The term "orientation" is used when we distinguish between views of a structure from front or back. The term "polarity" distinguishes "up" and "down." For example, when we invert the orientation of a chevron, the left and right sides are interchanged but the polarity remains the same; when a helix is turned upside down, the polarity is inverted but the helix hand stays the same, etc. In most diagrams we use a standard representation of an outer doublet microtubule as viewed from inside, distal end up. Thus the A-tubule is on the left, the B-tubule is on the right, and the inner junction faces towards the observer. To interpret the electron micrographs in absolute terms, we adhere to the following conventions: the copper grid is coated with carbon shiny side up, protein solution place on carbon. The grid is placed into the holder with coated side up, its orientation is then inverted upon entry into the microscope (side entry stage, Philips CM12). The film sees the electrons with emulsion side up, the number on the film is legible when facing the emulsion side (in the CM12). Thus, when the number is legible on the film or on the print, the view is effectively down from the top of the EM, with particles seen through the carbon support, i.e., when the surface of a microtubule wall touches

the carbon support, it also faces toward the observer. Since the 3-start helix of microtubules is left-handed, the striations run up and to the left when the outside of a microtubule wall touches the carbon. When the orientation of an opened up microtubule wall is inverted (inside toward the carbon support), the striations run up and to the right. Two juxtaposed microtubule walls with opposite orientations will thus generate chevrons whose polarity depends on how they were generated (details later, see Fig. 7).

Results

Lattices of Outer Doublet Microtubules (A and B)

Outer doublet microtubules contain one complete microtubule of 13 protofilaments (A-tubule) and one incomplete

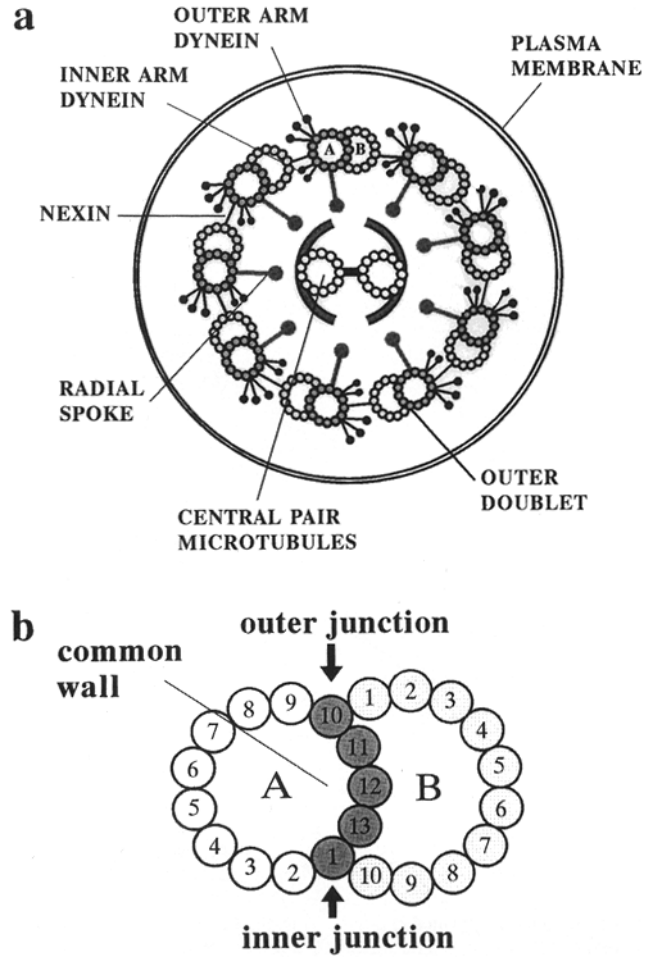

Figure 1. (*a*) Schematic cross section through flagellum, showing the nine outer doublet microtubules (*A* and *B*), two central pair microtubules, with associated components (dynein, nexin, and radial spokes). The view is from the flagellar tip towards the base, such that the B-tubule is on the clockwise side of the A-tubule. As a reference orientation we choose a view where the outer doublets are seen from inside the flagellum (i.e., A-tubule to the left of B-tubule, and tip of flagellum up) (i.e., as if the observer was standing on the basal body, inside the flagellum, plus end pointing up, minus end pointing down). (*b*) Magnified view of outer doublet cross section in standard orientation, with protofilaments numbered (after Linck et al., 1981). The inner junction between A- and B-tubules is formed by protofilaments A1-B10, the outer junction is formed by protofilaments A10-B1. Protofilaments A10-A1 (*dark shade*) form the common wall between A- and B-tubules. For simplicity we have omitted protofilament B11 which is seen only occasionally.

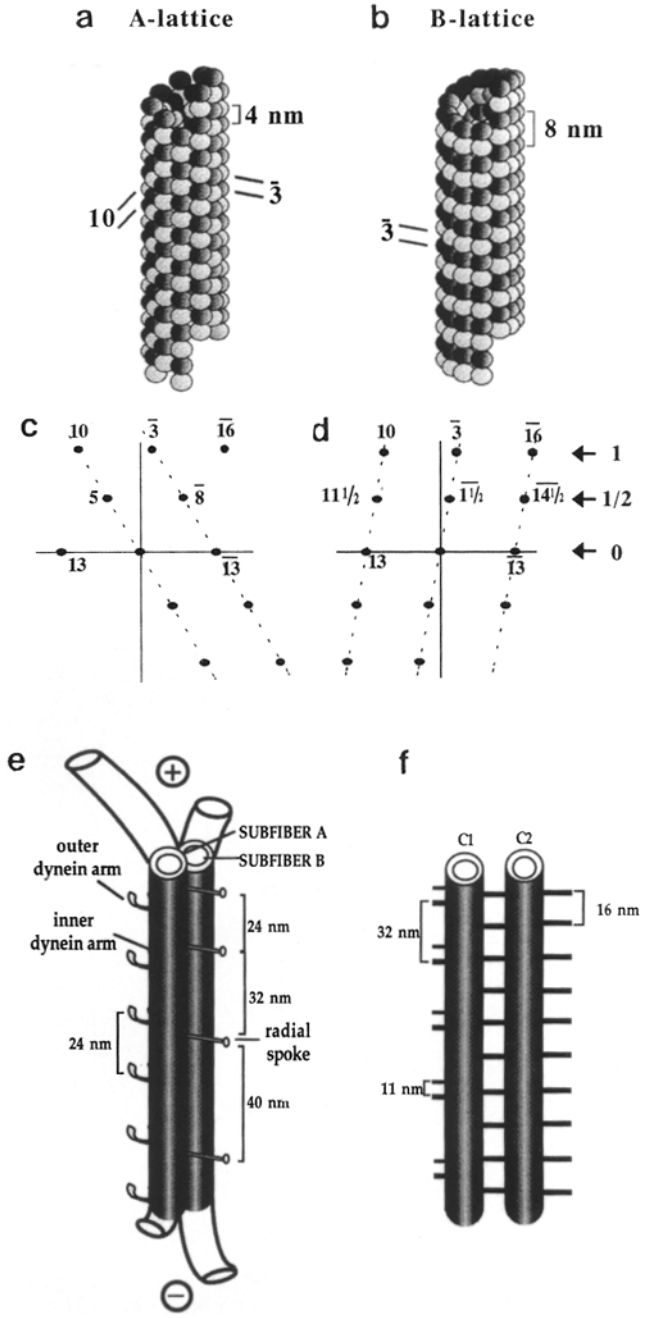

Figure 2. (*a*) Model of microtubule lattice A (helically symmetric, α- and β-tubulin alternate along 3-start helix); (*b*) B-lattice (α- or β-tubulin subunits are aligned along 3-start helix, except at a discontinuity where α meets β). (*c* and *d*) Simplified optical diffraction patterns of A- and B-lattice. Bessel orders indicating the helix multiplicities are indicated. The A-lattice (*c*) generates a reflection midway between the origin and the J_{10} term on the 4-nm layer line, and other orders thereof; the B-lattice (*d*) generates a reflection midway between the origin and the J_{-3} reflection. (*e*) Diagram of flagellar outer doublet (*A* + *B*) and (*f*) central pair C1 and C2 microtubules. In the EM the outer doublets can be recognized because they appear as paired microtubules, and because they can be elongated by added brain tubulin, as indicated by the extensions of the solid tubules. The plus end (distal end) grows faster (especially the A-tubule) and nucleates growth at a lower tubulin concentration. Central pair microtubule C1 can be recognized by irregular side arms (remaining from the paired projections with distance ≈11 nm and periodicity ≈32 nm) and mottled staining, C2 has more regular projections with ≈16 nm periodicity (see Linck et al., 1981).

microtubule of 10 (sometimes 11) protofilaments. In our standard view (from tip to base, Fig. 1) the B-tubule follows A in the clockwise direction. Dynein arms and radial spokes are attached to the A-tubule, pointing anti-clockwise (for review see Murray, 1991; Witman, 1992). In negative stain electron micrographs of isolated axonemes, the doublet microtubules can be recognized by their close juxtaposition and the attachment of dynein arms. The A-tubule tends to be longer than the B-tubule, especially at the distal end. Because of their polarity the microtubules have two distinct ends, plus (distal) and minus (proximal, Euteneuer and McIntosh, 1981). They can be distinguished by the growth rates when exogenous brain tubulin is added to the axonemes (Fig. 3); plus ends grow faster and require a lower tubulin concentration for growth (Bergen and Borisy, 1980).

Optical diffraction patterns of A- and B-tubules marked out individually show the prominent equatorial and 4-nm reflections, but no or very weak reflections on the 8-nm layer line (not shown, see Song and Mandelkow, 1993). The innermost pair of reflections on the 4-nm layer line corresponds to the left-handed 3-start helix (J_{-3} Bessel terms, Fig. 2, *c* and *d*; see Amos and Klug, 1974). When these microtubules are decorated with kinesin head, a prominent 8-nm layer line appears (Figs. 3 and 4). Its innermost reflections are situated roughly half way toward the J_{-3} reflections, indicating that the dimers (now decorated with kinesin head on β-tubulin) follow the 3-start helix, as in the B-lattice. Since this is observed for both A- and B-tubules separately, we conclude that both types of microtubules have the B-lattice, in agreement with the earlier results (Song and Mandelkow, 1993).

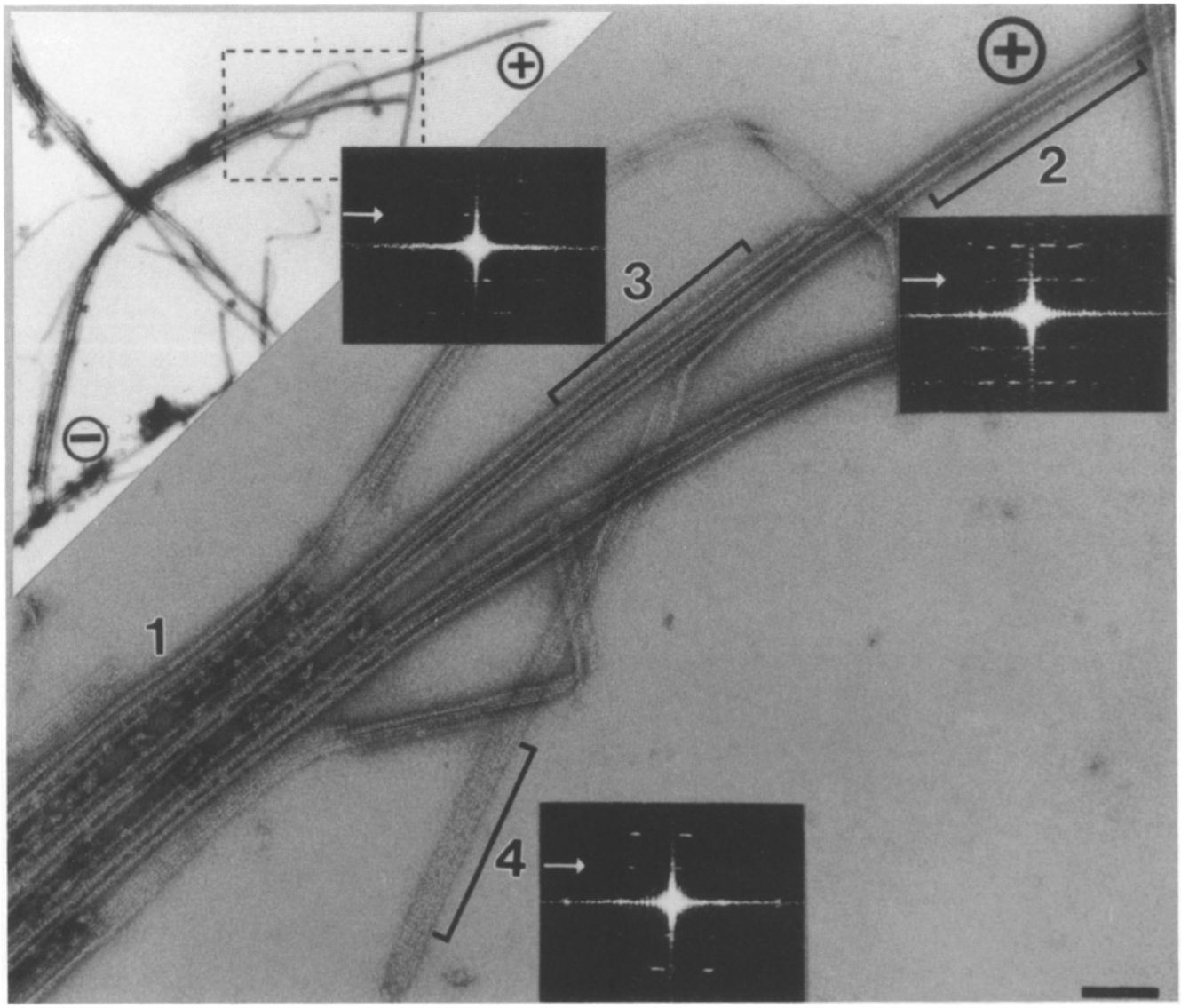

Figure 3. Kinesin-decorated axonemal outer doublet microtubules (*lower left*, with dynein arms attached) with porcine brain microtubule extensions (*toward upper right*, bare of dynein); the plus or fast-growing end points in the 2-o'clock direction. The insert, upper left, shows an overview of the whole assembly with extensions in the plus and minus directions; note that the plus-end extensions are much longer. One observes intact outer doublets (*1*), microtubule extensions from A-tubules (*2*) and B-tubules (*3*), and A-tubule extensions that have partially opened up, forming a sheet on the EM support (*4*). Inserts show representative optical diffraction patterns of the bracketed adjacent areas (from extended B-tubule, A-tubule, and sheet). All areas show 8-nm layer lines with reflections corresponding with B-lattice (*arrows*, for details see Fig. 5). Bar, 100 nm.

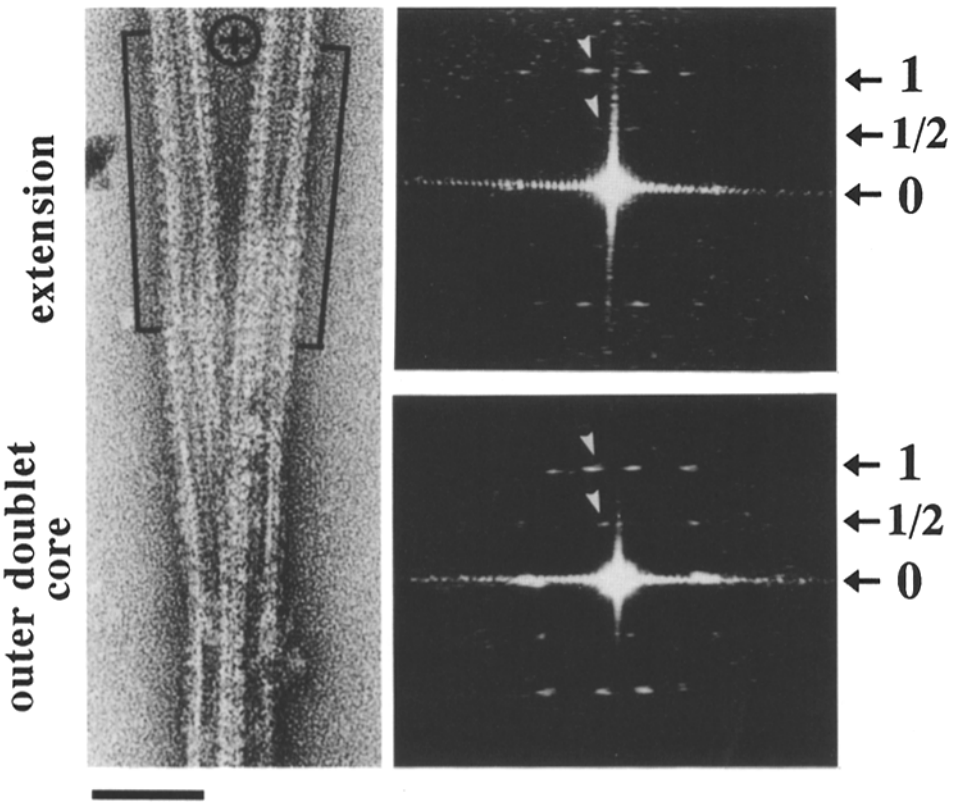

Figure 4. Electron micrograph (*left*) and diffraction patterns (*right*) of flagellar outer doublet microtubules and their extensions by porcine brain tubulin on the plus end in the presence of recombinant kinesin head. Diffraction patterns of the two bracketed areas show 4-nm and 8-nm layer lines with B-lattice reflections (*arrowheads*). Bar, 50 nm.

One technical problem in this approach is that the two microtubules lie very closely together, making it difficult to mask one of them out for analysis. We therefore made use of the fact that flagellar microtubules can be elongated by exogenous brain tubulin, as diagrammed in Fig. 2 *e* and shown in Figs. 3 and 4. The presence of a flagellar microtubule template is known to enhance the fidelity of the microtubule lattice in terms of protofilament number. For example, microtubules made by self-nucleation of brain tubulin frequently have 14 protofilaments or more, while the same tubulin added onto flagellar microtubule seeds or other microtubule-organizing structures generates 13-protofilament microtubules (Scheele et al., 1982; Evans et al., 1985). For our purpose this approach has several advantages. Depending on the concentration of added tubulin one can grow either the plus end alone, or plus and minus ends at different rates, and thus analyze the two extensions separately. Furthermore, the extended A- and B-tubules often do not stay together, making it possible to observe extended A- and B-tubules separately (Fig. 3, *top*). Finally, the extended microtubules often open up into sheets flattened on the carbon support, similar to microtubules made from brain tubulin (Fig. 3, *bottom*). These are two-dimensional crystals whose analysis no longer suffers from flattening and spurious edge effects of microtubule cylinders (Erickson, 1974).

A doublet with brain microtubule extensions on the plus end is shown in Fig. 4. Without the kinesin decoration, the optical diffraction patterns contain the usual 4-nm layer line but not the 8-nm layer line. However, with decoration, there is a new 8-nm layer line compatible with the B-lattice (Fig. 4). The same results are obtained for extended minus ends (not shown). Finally, Fig. 5 shows an example of two juxtaposed sheets emanating from doublet microtubule seeds; the cross-striations form a chevron pattern pointing in the plus direction. The diffraction patterns are crisp and contrasty, and again the positions of the peaks are those of the B-lattice. All of this data indicates that flagellar outer doublet microtubules contain only the B-lattice, both in their proximal and distal domains, both for A- and B-tubules, and independently of other flagellar proteins that are still attached to them.

Lattice of Central Pair Microtubules

The analysis of the dimer lattice of central pair microtubules poses the same problems as other microtubules; the arrangement of monomers shows the usual features (13 protofilaments, 3-start, and 10-start helices, etc.), but dimers are difficult to visualize because of their low intrinsic contrast. Since the central pair microtubules are singlets, and since 13 protofilaments would allow a symmetric A-lattice, it had generally been assumed that they indeed have the A-lattice. However, this is not the case.

Central pair microtubules differ from outer doublet microtubules not only in that they are singlets, but also by their decoration with other flagellar components (diagrammed in Fig. 2 *f*). As shown by Linck et al. (1981), the C1 tubule has pairs of projections repeating every 32 nm along the axis and separated by ≈11 nm; this order, however, is only poorly preserved in negative stain. The C2 tubule retains a fairly regular set of projections repeating every 16 nm. As expected, these features show up in the optical diffraction patterns as additional layer lines at 32 nm and/or 16 nm (Fig.

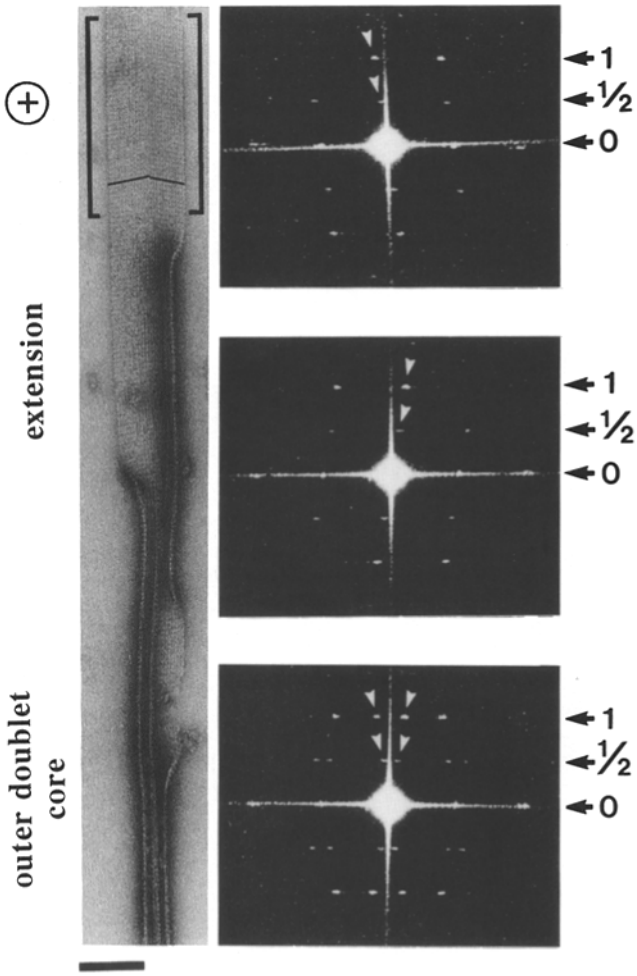

Figure 5. Tubulin sheet (*left, top*) emanating from outer doublet (*left, bottom*), decorated with kinesin head. The optical diffraction patterns of the bracketed area show the B-pattern particularly clearly since the sheet is a flat two-dimensional crystal, and since there is no overlap between the near and far side of a microtubule. The sheet shown here consists of two domains in opposite orientations, recognizable by the chevron pattern generated by the flattened 3-start helices (*highlighted by black lines*, for details see Mandelkow and Mandelkow, 1979; note that the chevrons point in the plus direction). The optical diffraction pattern of the composite sheet resembles that of a microtubule in that it is roughly symmetric about the meridian (since the "front" and "back" side lie next to one another, *bottom right*). However, the optical diffraction patterns from the individual domains are one-sided (*top right*, pattern from left domain; *middle right*, pattern from right domain indicated by the brackets). Bar, 100 nm.

6, *top*); by contrast, the reflections on the 8- and 4-nm layer lines are relatively weak.

When decorating axonemes with kinesin head and searching for central pair microtubules we noted two surprising features: normally it is difficult to identify the central pair microtubules because they tend to be buried and outnumbered by the outer doublets and associated material. However, decoration with kinesin head results in a loss of cohesion so that the central pair microtubules become individually visible. Moreover, they lose their thick cover of associated material so that the protofilament structure becomes much more clearly visible. This suggests that the kinesin head competes with and displaces most of the endogenous components (except for the 16-nm projections from C2). When decorated, both central pair microtubules show the oblique striations at 10° and the enhanced 8- and 4-nm layer lines indicative of the B-lattice (Fig. 6, *bottom*). This is a further generalization that the B-lattice is a common property of microtubules.

In this context it is worth noting that flagellar microtubules react with kinesin at all; evidently the kinesin-binding site is preserved in all of these tubulins (even though the flagellar motor is dynein and not kinesin). This would be consistent with the proposal of Goldsmith et al. (1991) that the sequence 422-436 conserved within all β-tubulins is the attachment site for kinesin, with the finding that the kinesin head cross-links preferentially with β-tubulin (Song and Mandelkow, 1993), and with the occurrence of kinesin-like molecules in flagella (Bernstein et al., 1994).

Junctions, Stagger, and Seam

Many opened up double microtubules had the appearance of Fig. 5, i.e., one could distinguish the parts emanating from the A- and B-tubules (close to 13 or 10 protofilaments), often with some remaining curvature (as in the center of Fig. 5) and the chevrons formed by the cross-striations pointed toward the plus end (Fig. 5, *top*, for more examples see Figs. 8 and 10). Since the A-tubule must contain a seam, we were also searching for 4-nm "steps" in the cross-striations where two protofilaments would slip by an additional monomer (for illustration see Fig. 2 *b*). This was however not observed; the majority of juxtaposed sheets clearly had continuous striations running from the edge right through to the junction in the center. This suggested that the expected seam was either lost or somehow obscured.

This prompted us to consider in more detail the mechanism of microtubule growth from flagellar seeds (Fig. 7 *a*). Imagine that during elongation, or during staining for electron microscopy, the outer junction (A10-B1) is weaker than the inner one (A1-B10) and opens up, allowing the B-tubule to unfold and flatten. This would generate a sheet of 10 protofilaments (with the outside facing down in Fig. 7 *a*). To generate a flattened A-tubule with 13 protofilaments but still joined to the B-tubule one could proceed only in one of two ways. Either the A-tubule breaks within the common wall, say at A13-A1; this would allow the A-tubule to unfold and flatten. In solution the two parts would form a Greek omega in cross section (Fig. 7 *a*, *bottom right*). In negative stain they would form a wide sheet (close to 13+10 protofilaments) with both domains in the same orientation, i.e., there would be no chevron pattern. This case is very rarely observed. The other option is to open the A-tubule outside the common wall, say at A1-A2; this would lead to an anti-S shape in cross section (Fig. 7 *a*, *bottom left*, *boxed*). In negative stain the two flattened domains would have opposite orientations and form a chevron pattern pointing in the plus direction. This case is by far the most frequent one (examples in Figs. 5, 8, and 10, diagram in Fig. 7 *c*). Note that the polarity of the chevrons would not change if they came to lie on the grid with opposite orientation, just as the direction of an arrow does not depend on a rotation around its axis.

In principle, the same reasoning could be applied to the

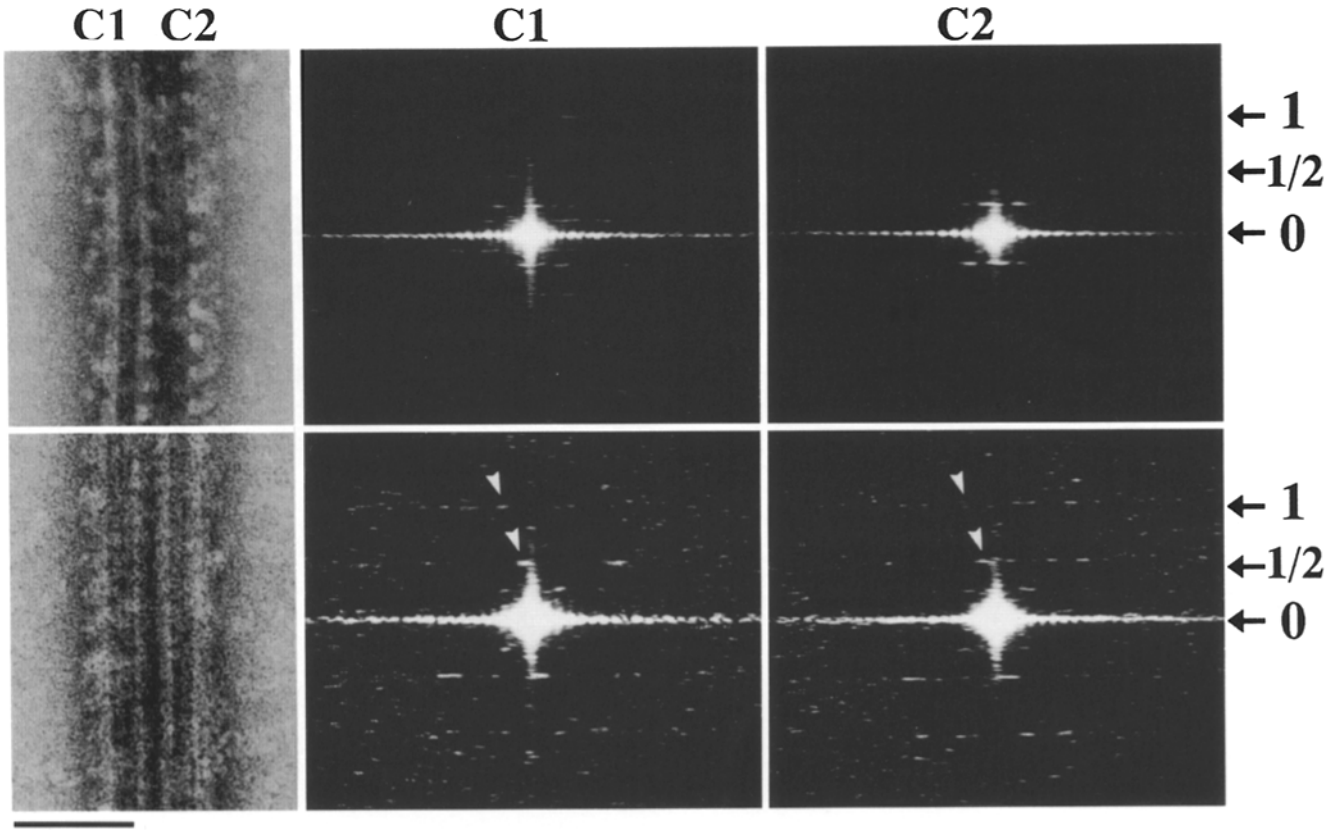

Figure 6. Central pair microtubules, C1 on left, C2 on right, undecorated (*top*) and decorated with kinesin head (*bottom*), with corresponding optical diffraction patterns. (*Top*) The C1 tubules have projections with a repeat of 32 nm, generating layer lines at orders of the repeat (32, 16, and 8 nm, *left pattern*). The C2 tubules have spiky projections with 16-nm repeats, generating prominent 16- and 8-nm layer lines (*right pattern*, for details see Linck et al., 1981). The 4-nm layer lines of the tubulin lattice are comparatively weak. (*Bottom*) Decoration with kinesin displaces much of the attached material. The 32-nm and most of the 16-nm layer lines disappear, but instead the 8-nm and 4-nm layer lines with the typical B-lattice of tubulin become enhanced (*arrowheads*). Bar, 50 nm.

case where the outer junction remains intact and the inner junction opens up (Fig. 7 *b*). Depending on how the second break at the A-tubule occurs one would form an anti-Omega or an S in cross section. An important difference is that the flattened S would have chevrons pointing in the minus direction—a case which is hardly ever observed. We conclude that the case of Fig. 7 *a* (*boxed*) is the one that explains the majority of our observations, implying that the inner junction is the one that remains intact, the outer one breaks, and the A-tubule breaks outside the common wall. This case is diagrammed in Fig. 7 *c*.

We return to the initial question: where is the seam? Given that the inner junction is the one that remains intact in the composite sheets, and given that the cross-striations run continuously across each domain without a step, the simplest explanation is that the seam must be where the A-tubule has opened up, i.e., between protofilaments A1 and A2. These two protofilaments are staggered not by 0.92 nm (as are all the others), but by 4–0.92 = 3.08 (see Fig. 7 *c*). Conversely, one could argue that the A-tubule opens up at the seam because this appears to be a weak spot; this may explain the reproducibility of the opened up sheets.

We can carry the analysis one step further and ask: what is the stagger between the A- and B-tubule at the inner junction A1-B10? This problem has been analyzed as follows (Fig. 8). The domains of the flattened A- and B-tubule were densitometered and the densities were summed up in the direction of the cross-striations (white chevron lines in Fig. 8, *top*). The projected density traces are shown below. The high peaks at 8-nm intervals show the β-tubulin–kinesin complex, the intervening lower densities represent α-tubulin. This allows the precise positioning of the density peaks (indicated by dots for β-tubulin). Next the maximum density lines were traced back to the junction between A and B (white dividing line in Fig. 8, *top*). The cross-striations from the two domains meet each other with a stagger of roughly half a dimer repeat, i.e., ~4 nm. This finding is indicated in Fig. 7 *c* (half stagger between protofilaments A1 and B10).

Fig. 7 *d* summarizes the above observations on the junctions and the seam. The darkly shaded part is the wall of the A-tubule seen from the inside of the B-tubule; the common wall is formed by protofilaments A10-A1. The junction protofilaments from the B-tubule are overlaid with lighter shade, B1 over A10 at the outer junction, B10 over A1 at the inner junction. At the outer junction, the dark α subunits roughly coincide in height. At the inner junction the α subunits are out of register. The seam is shown between A1 and A2.

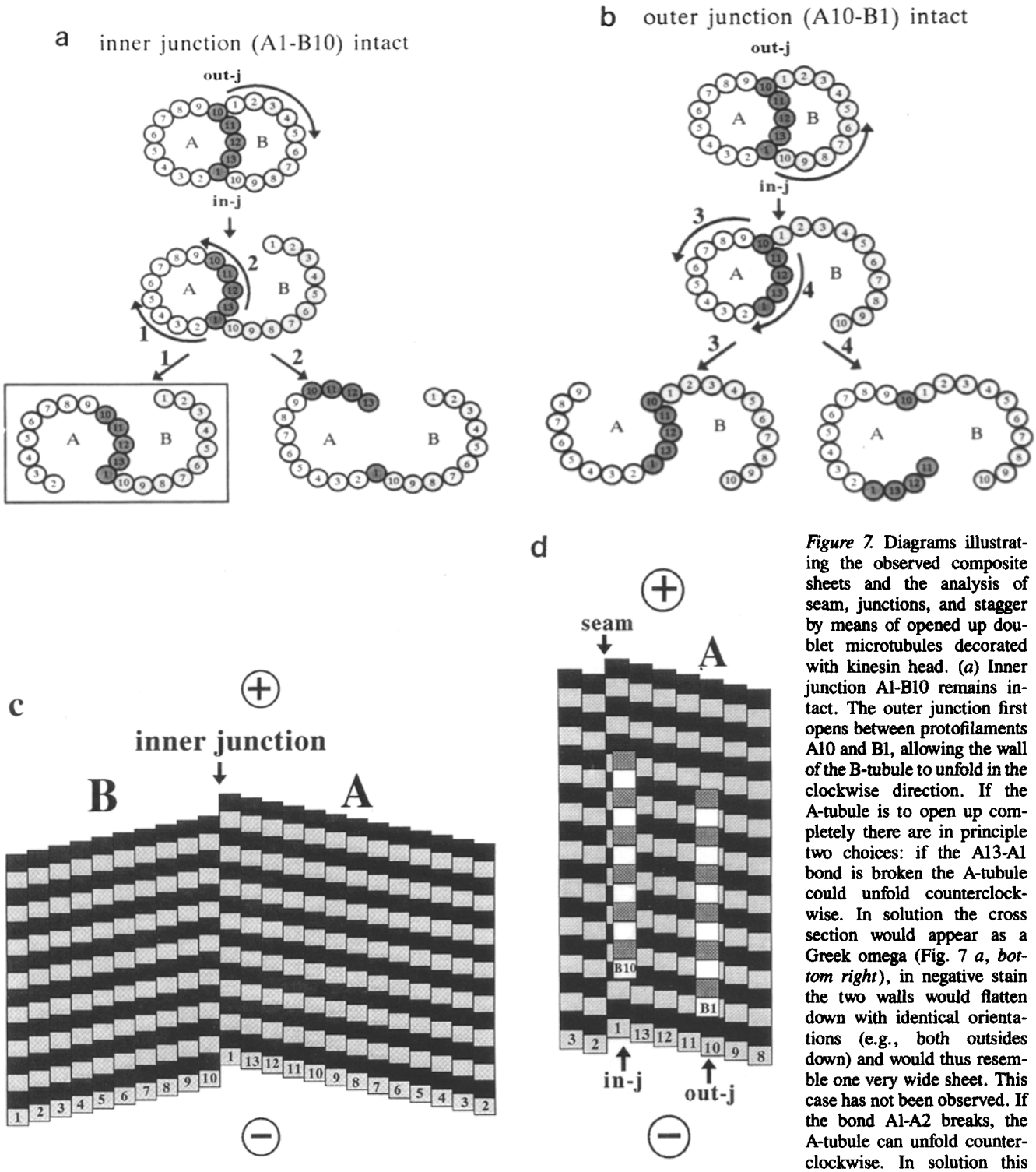

Figure 7. Diagrams illustrating the observed composite sheets and the analysis of seam, junctions, and stagger by means of opened up doublet microtubules decorated with kinesin head. (*a*) Inner junction A1-B10 remains intact. The outer junction first opens between protofilaments A10 and B1, allowing the wall of the B-tubule to unfold in the clockwise direction. If the A-tubule is to open up completely there are in principle two choices: if the A13-A1 bond is broken the A-tubule could unfold counterclockwise. In solution the cross section would appear as a Greek omega (Fig. 7 *a*, *bottom right*), in negative stain the two walls would flatten down with identical orientations (e.g., both outsides down) and would thus resemble one very wide sheet. This case has not been observed. If the bond A1-A2 breaks, the A-tubule can unfold counterclockwise. In solution this would form an anti-S-shape (*bottom left*, *boxed*), when flattened in negative stain it would appear as a composite sheet with opposite orientations, forming a chevron with arrows in the plus direction, as in Fig. 7 *c* below. This is the predominant case observed. (*b*) Outer junction A10-B1 remains intact. This case is the mirror image of Fig. 7 *a*, it could generate an omega (*bottom right*) or an S-shape, depending on whether bonds A10-A11 or A9-A10 are broken. However, in this case, the chevrons would point in the minus direction which is not observed. (*c*) Diagram of a flattened composite sheet, corresponding to the side view of the anti-S of Fig. 7 *a*, bottom left (*boxed*). The flattened A-tubule (*right*) has 13 protofilaments and is seen with its outside toward the observer (so that cross-striations run up and to the left, corresponding to the left-handed 3-start helix). The flattened B-tubule (*left*) has 10 protofilaments and is seen with its inside towards the observer (*cross-striations up and to the right*). The inner junction is formed by protofilaments A1-B10, the outer protofilaments are numbered as shown. If this structure came to lie on the grid with opposite orientation, the A- and B-tubules could still be distinguished by the number of protofilaments, and the direction of the chevrons would stay the same, towards the plus direction (convince yourself by viewing the diagram from the back of the page). Since only plus-end chevrons are observed this means that the inner junction is the strong one and the outer junction breaks easily (as in Fig. 7 *a*, *boxed*). This diagram also shows three features to be demonstrated below: the plus end terminates with α-tubu-

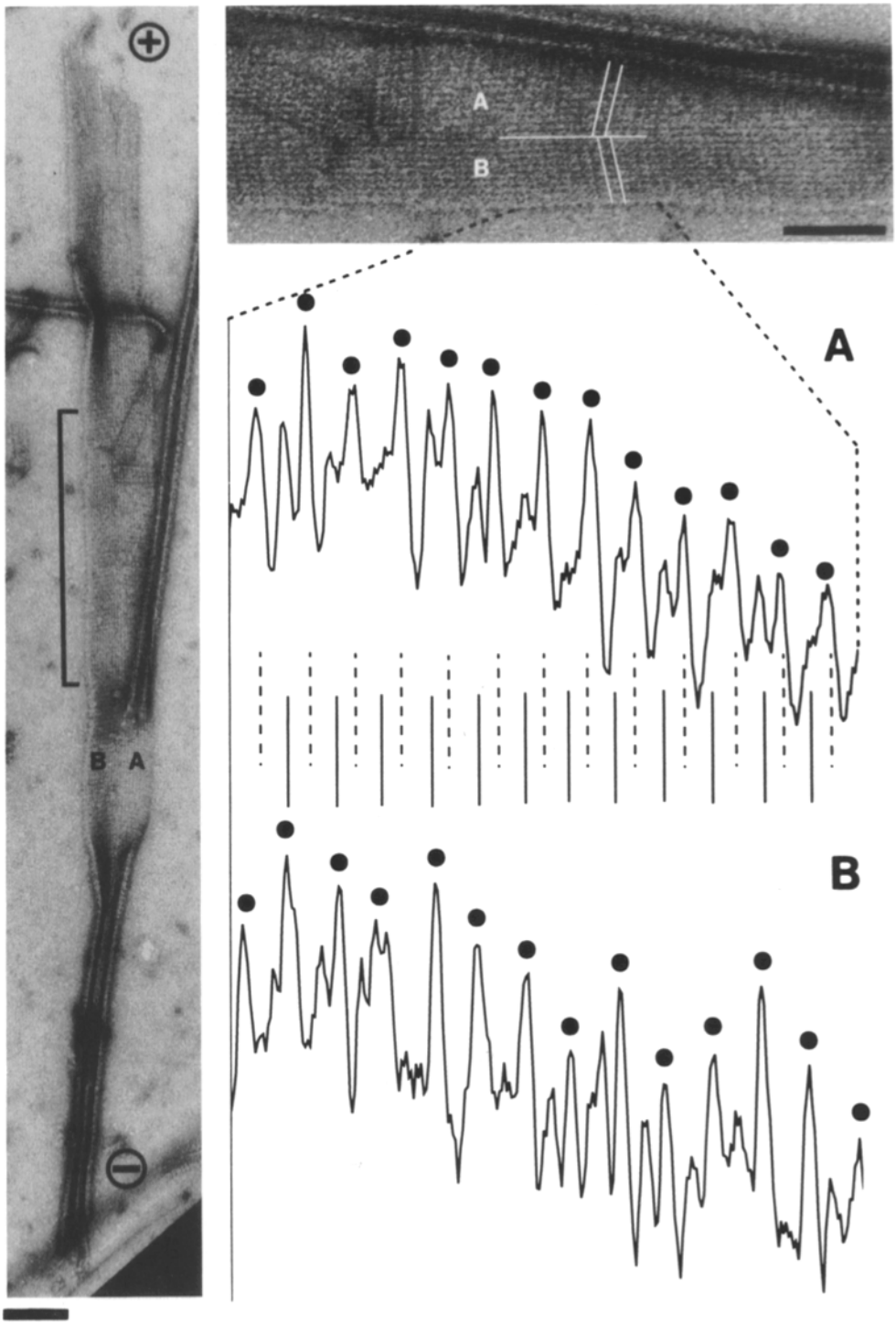

Figure 8. (*Left*) Opened up doublet tubule, plus end extension. The B-tubule with 10 protofilaments is on the left, oriented with inside towards carbon support so that cross-striations run up and to the right (note that this orientation tends to stain more darkly). The A-tubule with 13 protofilaments is on the right, with cross-striations running up and to the left. This generates chevrons pointing in the plus direction (as in Fig. 7 *c*). The boxed area is shown magnified on the top right, rotated by 90° (*plus end left*). The *A* and *B* areas were scanned, and the densities were superimposed in the direction of the cross-striations (indicated by *white chevron lines*), generating the density profiles shown below. The dots mark high densities (β-tubulin plus kinesin), and the intervening lower peaks are from α-tubulin. Note that the polarity can be identified, for example, by the fact that the deep cleft is on the minus side of β-tubulin; since this occurs in both the A- and B-tubule, they have the same polarity. When the iso-density lines are traced back to the junction (*white separating line*) they meet with a half-stagger (note interdigitating marks between density traces, *dashed* for the A-domain, *solid* for the B-domain). This means that the protofilaments of the inner junction, A1-B10, are staggered by about half a dimer, i.e., ≈4 nm (reminiscent of the seam to be described below). All bars, 100 nm.

lin, the inner junction protofilaments A1-B10 are staggered by about one tubulin monomer (≈4 nm), and the flattened walls do not show the helical discontinuity required by the lattice, implying that the discontinuity occurs between protofilaments A1 and A2, that is, the seam has the weak bonds and has opened up. (*d*) Diagram of the common wall and adjacent protofilaments of the A-tubule as they would be seen from inside the B-tubule. The B-protofilaments forming the junctions are superimposed (but the others omitted for clarity). The inner junction is on the left (A1-B10). Here the protofilaments are roughly half-staggered, i.e., an α-subunit of A1 (*dark shade*) faces a β subunit of B10 (*white*), and vice versa. The outer junction is on the right (A10-B1). Here the two protofilaments are roughly in phase (α subunits of A10 facing α subunit of B1). This follows from the surface lattice: between A10 and A1 the A-protofilaments shift up by 4×0.92 nm ≈ 3.7 nm, between B1 and B10 the B-protofilaments shift up by 9×0.92 nm ≈ 8.3 nm, the difference being $5 \times 0.92 \approx 4.6$ nm, which is close to the size of a monomer. Similarly, by applying this kind of reasoning to the A-tubule one can conclude that there must be a seam somewhere in the wall; since it is not observed in the fully flattened walls (see text) it probably lies where the walls open up, i.e., between protofilaments A1 and A2 as shown here (*seam*).

Polarity and Crown

The shape of the density profiles (as in Fig. 8) reveals yet another property, the polarity. This is best visualized by the dark stain-filled cleft adjacent to the bright density peak of β-tubulin. The deep cleft is on the minus side of β-tubulin (i.e., to the right of the dotted peaks in Fig. 8). This allows us to determine polarities even where the plus and minus ends are not known a priori (computer image processing to be shown elsewhere reveals this feature even more clearly). From the positions of the clefts and the peaks, we can conclude that the polarities of all microtubules analyzed here are the same (compare for example the two traces in Fig. 8). This confirms the data of Euteneuer and McIntosh (1981) who deduced the polarities from the sidedness of tubulin "hooks" polymerized onto flagellar microtubule walls.

We can now extend this analysis and ask: given that all protofilaments have the same polarity, what are the terminal subunits, α or β? This has been one of the most long-standing questions in microtubule structure, for reasons related to GTP exchange and microtubule dynamics (see Discussion). The two possibilities are diagrammed in Fig. 9. On the left the protofilaments have a crown of β subunits at the plus end, and α subunits at the minus end where they presumably interact with nucleating structures containing gamma tubulin. On the right the polarity of the dimer is inverted. The diagram also incorporates Mitchison's (1993) recent demonstration that exchangeable GTP is indeed bound to the β subunits at the plus end, while the interior of the microtubule contains GDP.

The analysis shown in Fig. 10 proceeded similar to that of Fig. 8. Opened up microtubule walls were scanned, the density superimposed along the cross-striations. The polarity was usually known from the lengths of the microtubule extensions (see overview in Fig. 10, *left*), but the polarity of the density profiles served as an additional check (note the deep clefts on the minus side of the β-tubulin peaks). We then followed the profiles to the very end, and invariably the plus end terminated with α-tubulin. Conversely the minus ends terminated with β-tubulin (not shown). This agrees with the model on the right of Fig. 9, and in the previous diagrams of Figs. 2 and 7, we have already anticipated the result (darkly shaded α-tubulin at the plus end).

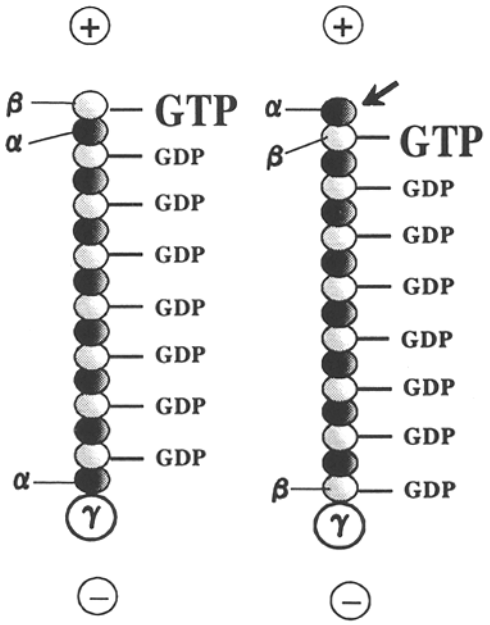

Figure 9. Two models of dimer polarity. (*Dark shade*) α-tubulin; *bottom*, minus end where γ-tubulin would be expected at nucleating sites. β-Tubulin subunits contain mostly hydrolyzed GDP, except at the plus ends where they have GTP (Mitchison, 1993). On the left, the protofilament ends with a β subunit at the plus end (as proposed by Mitchison, 1993). On the right, (*arrow*) the protofilament ends with an α subunit (as proposed by Oakley, 1992). This model is consistent with the data shown here (Fig. 10).

Discussion

Surface Lattice

The eukaryotic flagellum is a highly organized motile machinery and thus lends itself to a structural analysis by diffraction methods (for review see Murray, 1991; Witman, 1992). One prerequisite for understanding the function of any motor would be to know where the parts are. While much is known about the arrangements of the large components such as dyneins, spokes, nexins, and microtubules in general, it has been particularly difficult to identify the details of the microtubule lattices on which the various components are suspended. The reason is that it has been difficult to identify tubulin heterodimers, the building blocks of microtubules, because of their very low intrinsic contrast. A solution to the problem is the kinesin decoration technique, where β-tubulin is selectively enhanced by binding the recombinant kinesin head domain (Song and Mandelkow, 1993). Both in negative stain and cryo-electron microscopy the kinesin head binds with a spacing of 8 nm, indicative of the distance between tubulin dimers and a stoichiometry of one head per tubulin dimer (Song and Mandelkow, 1993; Harrison et al., 1993). This allows one to address several unresolved questions on flagellar microtubules: what are the lattices of A-, B-, and C-tubules? What is the structure of the two A-B junctions? Where is the seam in the A-tubule? Do all microtubules have the same polarities? What subunits do the crowns of the microtubules consist of?

In the models shown in most text books, it is assumed that the A-tubules have the A-lattice which allows full cylindrical symmetry, and B-tubules have the B-lattice, following the work of Amos and Klug (1974). Although the B-lattice does not allow cylindrical symmetry for a 13-protofilament microtubule, this is not a conceptual problem for the B-tubule since this is not a complete tubule anyway. Finally, the central pair tubules were assumed to have the A-lattice as well since they are complete 13-protofilament microtubules, although Linck et al. (1981) already pointed out that the situation might be more complicated. Our results are simply summarized by stating that all flagellar microtubules have the B-lattice, both at their proximal and distal ends. This makes them similar to the cytoplasmic microtubules which also have the B-lattice, as shown earlier (Song and Mandelkow, 1993). This is illustrated in Fig. 11 which represents models of outer doublets and central pair microtubules, with some of their associated motors or cross bridges attached.

The B-lattice is found not only with flagellar microtubules, but also in the extensions generated by adding brain tubulin.

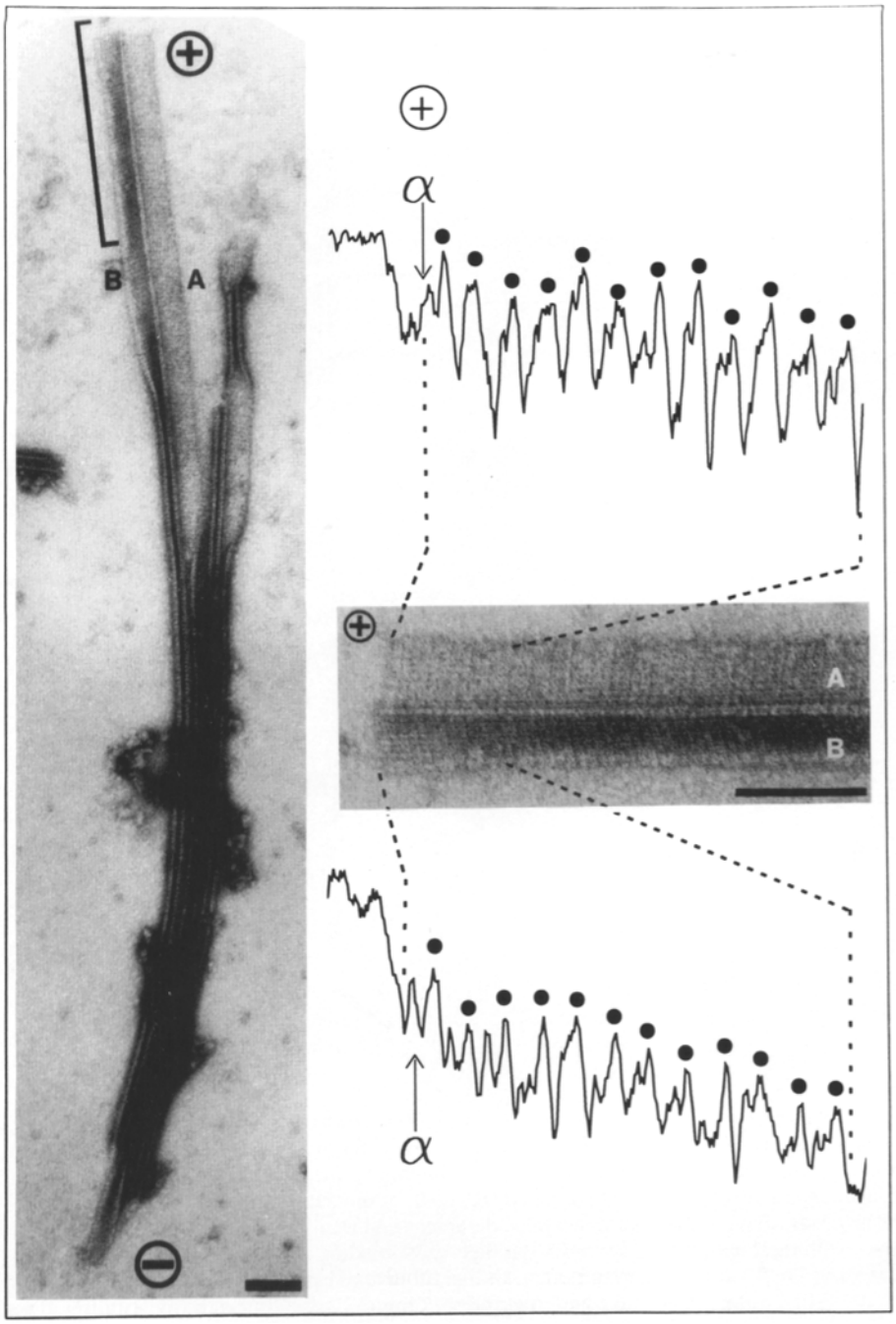

Figure 10. Projected density at the plus end of an opened up microtubule. (*Left, overview*) B-tubule on the left, A-tubule on the right (with some curvature retained), and chevrons in plus direction (see Fig. 7 *c*). Boxed area is shown magnified on right, turned by 90°. The projected densities along the cross-striations of the two halves (excluding the curved central part) are shown above and below. The polarities of the two halves are the same, as in Fig. 7 (deep cleft on the minus side of the high density of β-tubulin plus kinesin, *marked by dots*). In both cases there is a clear intermediate peak of α-tubulin at the end. Similar scans along minus ends show that they terminate with β-tubulin (not shown). This is the polarity shown in Fig. 9 on the right. Bars, 100 nm.

When flagellar microtubules are used as seeds, the plus end tends to grow faster than the minus end (especially the A-tubule, as diagrammed in Fig. 2 *e*) which allows one to distinguish between the two ends. The fact that both extensions have the same lattice as the body of the axonemal microtubule illustrates that the structural fidelity is preserved at the level of the surface lattice. This nicely complements earlier studies which showed that natural seeds such as axonemes or centrosomes conserved the number of 13 protofilaments while self-nucleated brain tubulin often has 14 or more protofilaments (Scheele et al., 1982; Evans et al., 1985; for a recent review see Wade and Chretien, 1993).

In this context one should mention the lattice terminology currently in use—A, B, and mixed. The A- and B-lattices were defined by Amos and Klug (1974) (see Fig. 2, *a* and *b*). When a microtubule wall with a B-lattice is closed this generates a seam with an A-type structure (as in Fig. 2 *b*). We refer to this as a B-lattice since the B-type interaction predominates; McEwen and Edelstein (1980) called the same arrangement a mixed lattice, emphasizing that both types of interactions occurred in the same microtubule (see their Fig. 1). More recently, the term "mixed lattice" was used by Wade and Chretien (1993) to mean a random mixture of A-type and B-type interactions. While theoretically possi-

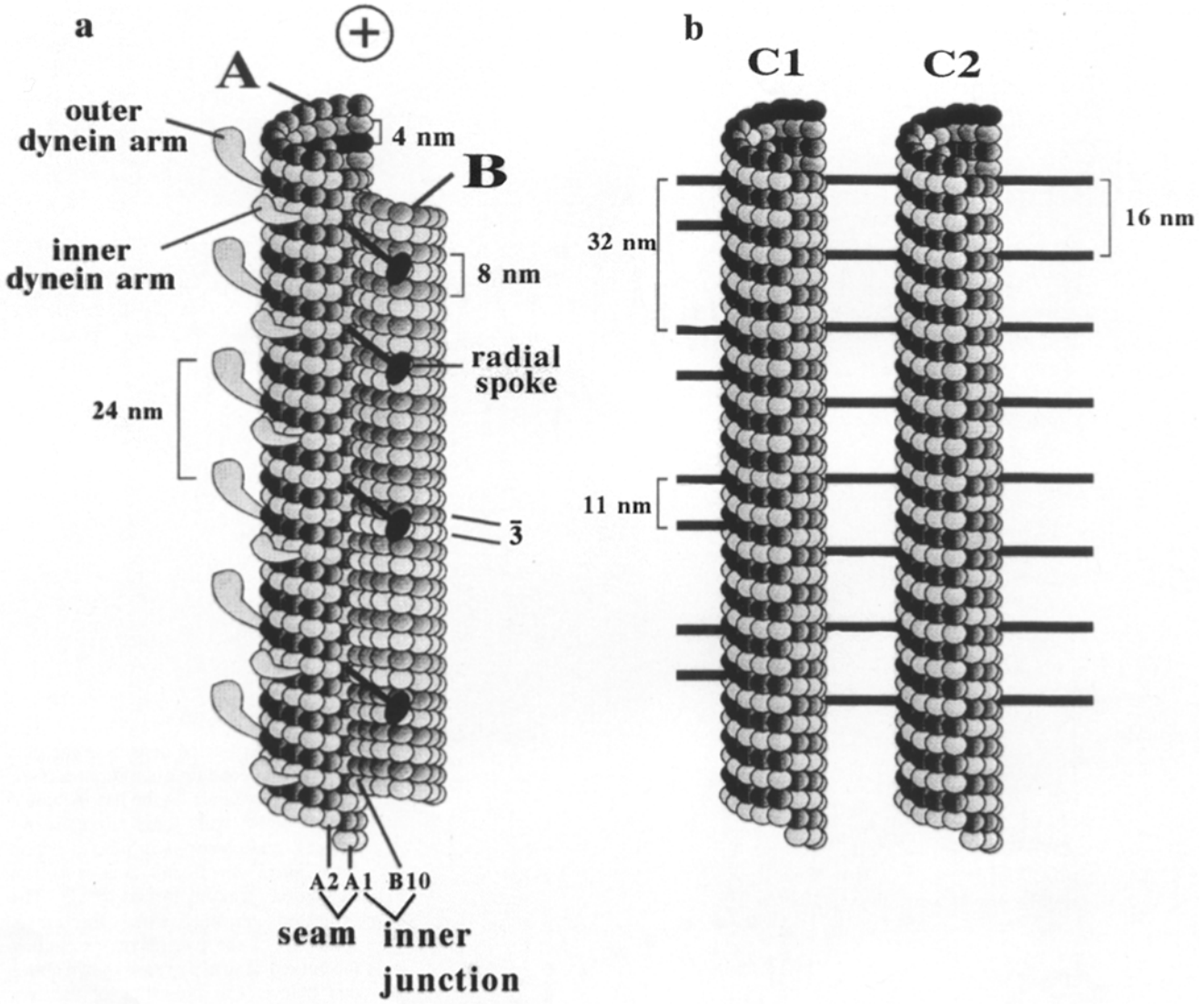

Figure 11. Models of outer doublet and central pair microtubules summarizing the data shown here. (*a*) (*Outer doublet*) Both tubules have a B-lattice, and both have the same polarity. The inner junction (A1-B10, *facing us*) is strong, the outer junction is weaker and opens more easily. The A-tubule has a seam between protofilaments A1 and A2 which are staggered roughly by half a dimer (so that α faces β and vice versa). The protofilaments at the inner junction are also roughly half-staggered (A1-B10), at the outer junction (A10-B1, not visible here) they are roughly in phase. The plus end terminates with a crown of α subunits, the minus end terminates with β subunits. The non-tubulin components (dynein, spokes) are drawn with their appropriate spacings, but their exact binding sites on the microtubule are unknown. (*b*) Central pair microtubules. They also have the B-lattice, requiring a seam. C1 and C2 tubules can be distinguished by the spacing of their associated components (see Linck et al., 1981). Since opened up central pair tubule extensions are difficult to identify it was not possible to determine the position of the seam relative to the associated components or relative to the C1-C2 axis, so its position is shown arbitrarily.

ble, this model is actually not observed experimentally. Note that with a random mixture the 8-nm layer line would tend to disappear since the 8-nm periodicity would be averaged out.

The results described here imply that decorated microtubules have a stoichiometry of 1 kinesin head per tubulin dimer, as mentioned above. Secondly, our chemical cross-linking experiments showed that the kinesin head binds preferentially to β- but not α-tubulin, consistent with the suggestion of Goldsmith et al. (1991) that the conserved region β422-436 is involved in kinesin binding. These structural results can be compared with the movement of kinesin along microtubules. The path appears to follow the direction of the protofilaments (rather than crossing between protofilaments, see Kamimura and Mandelkow, 1992; Ray et al., 1993). This implies that the step sizes should be 4 nm (= repeat of monomers), 8 nm (= repeat of dimers), or multiples thereof. Measured step sizes of kinesin of dynein along microtubules have major components at 8-nm spacing, consistent with the tubulin dimer repeat (Kamimura and Kamiya, 1992; Svoboda et al., 1993). On the other hand, step components with 4-nm spacing have been observed as well, indicating that during motion the tubulin monomers may play a role irrespective of the difference between α- and β-tubulin (Gelles et al., 1988; Kamimura and Kamiya, 1992). The variability

might be explained by assuming that a moving target is different from a stationary one, i.e., a kinesin molecule traveling along a microtubule might be able to touch down transiently on α- or β-tubulin, but would prefer β-tubulin as a resting site. In addition, one should note that the dynamic experiments are done at very low kinesin/tubulin ratios whereas the ratio is high in our case, allowing possibly for interactions between kinesin molecules on the microtubule surface.

Seam and Junctions

If the A-tubule has a B-lattice, then it must also have a seam—but where is it? Opened up microtubules have provided the answer; the seam is not seen in the flattened walls of A- and B-tubules; on the contrary, the cross-striations are continuous across the domains. Thus the seam must be placed near the inner junction, between protofilaments A1 and A2. This conclusion is based on the reproducibility of the structure and polarity of the opened up walls. It can be explained only by assuming that the inner junction stays intact, and that the A-tubule opens up at the seam. This would mean that the seam is a potentially weak spot in the microtubule wall, not a strong one. The function of the seam remains obscure; it could be an attachment point, or it could simply be a point where the final closure of a microtubule occurs during growth, or a preferential point of disassembly. In the flagellum the stability or instability of junctions and seams could be modulated by additional proteins, for example the tektins which are known to bind along the length of microtubules (Steffen and Linck, 1988).

The stagger between A- and B-tubules can be determined directly for the case of the inner junction—it is ~4 nm, i.e., the dimers in protofilaments A1 and B10 are roughly half staggered. For the outer junction this implies that the dimers must be roughly in phase (Fig. 7 *d*). Thus the two junctions are unequal, not only in sidedness (the bonding involves different sides of the protofilaments, Figs. 7 and 11), but also in stagger. We note here that the hook decoration technique in high Pipes buffer generates clockwise hooks when viewed in our standard orientation (and thus can be used to determine polarities, Euteneuer and McIntosh, 1981). The hook junction is therefore equivalent to the outer junction (since the B-tubule curves away from the outer junction in a clockwise fashion).

Polarity

Perhaps the most surprising result was that the plus end of a microtubule has a crown of α-tubulin subunits. In the past there have been a number of unsuccessful attempts to answer this problem, the difficulty being again the lack of contrast between α- and β-tubulin. The question of the crown played a fundamental implicit role in many publications on microtubule dynamics (for reviews see Mandelkow and Mandelkow, 1989; Erickson and O'Brien, 1992). The reason is that tubulin is activated for assembly by GTP binding to β-tubulin; upon attachment the GTP is hydrolyzed so that the interior of a microtubule contains only GDP. Thus the "GTP cap hypothesis" (Hill and Chen, 1984) tacitly assumed that an exchange of GTP was possible at the terminal β subunits of the active (plus) end of a microtubule. The size of the cap was a matter of debate, but recently Mitchison (1993) confirmed directly that GTP was bound near the plus end. This would be explained neatly if the plus end had a crown of β subunits, as shown in Fig. 9 (*left*). However, the opposite model was suggested by Oakley (1992); he observed a genetic linkage between γ-tubulin and β-tubulin, and since γ-tubulin is involved in microtubule nucleation at the minus end, the crown of β subunits was thought to be at the minus end while the plus end would then have a crown of α subunits (Fig. 9, *right*). This is what we have observed here.

The consequence for models of nucleotide exchange and dynamic instability is that β-tubulin·GTP is never at the very end of a microtubule plus end. As soon as a dimer associates, the β subunit is already internal, covered by another α subunit. To explain the presence of GTP at that end, one has to postulate that the nature of the terminal dimer is different as a whole from dimers further inside a microtubule. Considering the flexibility of proteins and of tubulin in particular, it is not difficult to imagine a situation where the terminal dimer is more loosely bound, even though the β subunit is already internal.

We are grateful to Dr. Ken Kosik for the cDNA clone of squid kinesin, Dr. Alexander Marx for help with image processing, Jens Müller for photography, and Dr. Eva-Maria Mandelkow for advice and stimulating discussions. Sea urchins were made available by the Biologische Bundesanstalt Helgoland.

The project was supported by the Bundesministerium für Forschung und Technologie and the Deutsche Forschungsgemeinschaft.

Received for publication 7 February 1994 and in revised form 5 October 1994.

References

Amos, L. A., and A. Klug. 1974. Arrangement of subunits in flagellar microtubules. *J. Cell Sci.* 14:523–549.

Bell, C., C. Fraser, W. Sale, W.-J. Tang, and I. R. Gibbons. 1982. Preparation and purification of dynein. *Methods Cell Biol.* 24:373–397.

Bergen, L. G., and G. G. Borisy. 1980. Head-to-tail polymerization of microtubules in vitro. *J. Cell Biol.* 84:141–150.

Berstein, M., P. L. Beech, S. G. Katz, and J. L. Rosenbaum. 1994. A new kinesin-like protein (klp1) localized to a single microtubule of the *Chlamydomonas* flagellum. *J. Cell Biol.* 125:1313–1326.

Bloom, G. S. 1992. Motor proteins for cytoplasmic microtubules. *Curr. Opin. Cell Biol.* 4:66–73.

Brady, S. T. 1985. A novel brain ATPase with properties expected for the fast axonal transport motor. *Nature (Lond.).* 317:73–75.

Crepeau, R. H., B. McEwen, and S. J. Edelstein. 1978. Differences in alpha and beta polypeptide chains of tubulin resolved by electron microscopy with image reconstruction. *Proc. Natl. Acad. Sci. USA.* 75:5006–5010.

Erickson, H. P. 1974. Microtubule surface lattice and subunit structure and observations on reassembly. *J. Cell Biol.* 60:153–167.

Erickson, H. P., and E. T. O'Brien. 1992. Microtubule dynamic instability and GTP hydrolysis. *Annu. Rev. Biophys. Biomol. Struct.* 21:145–166.

Euteneuer, U., and J. R. McIntosh. 1981. Polarity of some motility-related microtubules. *Proc. Natl. Acad. Sci. USA.* 78:372–376.

Evans, L., T. Mitchison, and M. Kirschner. 1985. Influence of the centrosome on the structure of nucleated microtubules. *J. Cell Biol.* 100:1185–1191.

Gelles, J., B. J. Schnapp, and M. P. Sheetz. 1988. Tracking kinesin-driven movements with nanometre-scale precision. *Nature (Lond.).* 331: 450–453.

Gibbons, I. R., and E. Fronk. 1979. A latent adenosine triphosphatase form of dynein I from sea urchin sperm flagella. *J. Biol. Chem.* 254: 187–196.

Goldsmith, M., J. Connolly, N. Kumar, J. Wu, L. Yarbrough, and D. Vanderkooy. 1991. Conserved beta-tubulin binding domain for the microtubule-associated motors underlying sperm motility and fast axonal transport. *Cell Motil. Cytoskeleton.* 20:249–262.

Goldstein, L. S. B. 1991. The kinesin superfamily: tails of functional redundancy. *Trends Cell Biol.* 1:93–98.

Harrison, B., S. Marchese-Ragona, S. Gilbert, N. Cheng, A. Steven, and K. A. Johnson. 1993. Decoration of the microtubule surface by one kinesin head per tubulin heterodimer. *Nature (Lond.).* 362:73–75.

Hill, T. L., and Y.-D. Chen. 1984. Phase changes at the end of a microtubule with a GTP cap. *Proc. Natl. Acad. Sci. USA.* 81:5772–5776.

Huang, T. G., J. Suhan, and D. D. Hackney. 1994. Drosophila kinesin motor

domain extending to amino-acid position 392 is dimeric when expressed in *Escherichia coli*. *J. Biol. Chem.* 269:16502–16507.

Kamimura, S., and R. Kamiya. 1992. High-frequency vibration in flagellar axonemes with amplitudes reflecting the size of tubulin. *J. Cell Biol.* 116:1443–1454.

Kamimura, S., and E. Mandelkow. 1992. Tubulin protofilaments and kinesin-dependent motility. *J. Cell Biol.* 118:865–875.

Kosik, K. S., L. D. Orecchio, B. Schnapp, H. Inouye, and R. L. Neve. 1990. The primary structure and analysis of the squid kinesin heavy-chain. *J. Biol. Chem.* 265:3278–3283.

Kuznetsov, S., Y. Vaisberg, S. Rothwell, D. Murphy, and V. I. Gelfani. 1989. Isolation of a 45-kda fragment from the kinesin heavy-chain with enhanced ATPase and microtubule-binding activities. *J. Biol. Chem.* 264:589–595.

Linck, R. W., G. E. Olson, and G. L. Langevin. 1981. Arrangement of tubulin subunits and microtubule-associated proteins in the central-pair microtubule apparatus of squid sperm flagella. *J. Cell Biol.* 89:309–322.

Linck, R. W., and G. L. Langevin. 1981. Reassembly of flagellar B($\alpha\beta$) tubulin into singlet microtubules: consequences for cytoplasmic microtubule structure and assembly. *J. Cell Biol.* 89:323–337.

Mandelkow, E.-M., and E. Mandelkow. 1979. Junctions between microtubule walls. *J. Mol. Biol.* 129:135–148.

Mandelkow E., and E.-M. Mandelkow. 1989. Tubulin, microtubules, and oligomers: molecular structure and implications for assembly. *In* Cell Movement. Vol. 2. F. D. Warner and J. R. McIntosh, editors. A. R. Liss, New York. 23–45.

Mandelkow E. M., E. Mandelkow, P. N. T. Unwin, and C. Cohen. 1977. Tubulin hoops. *Nature (Lond.)*. 265:655–657.

Mandelkow, E.-M., R. Schultheiss, R. Rapp, M. Müller, and E. Mandelkow. 1986. On the surface lattice of microtubules: helix starts, protofilament number, seam, and handedness. *J. Cell Biol.* 102:1067–1073.

McEwen, B., and S. Edelstein. 1980. Evidence for a mixed lattice in microtubules reassembled in vitro. *J. Mol. Biol.* 139:123–145.

Mitchison, T. J. 1993. Localization of an exchangeable GTP-binding site at the plus end of microtubules. *Science (Wash. DC)*. 261:1044–1047.

Murray, J. M. 1991. Structure of flagellar microtubules. *Int. Rev. Cytol.* 125:47–93.

Oakley, B. R. 1992. Gamma-tubulin: the microtubule organizer? *Trends Cell Biol.* 2:1–5.

Ray, S., E. Meyhofer, R. A. Milligan, and J. Howard. 1993. Kinesin follows the microtubules protofilament axis. *J. Cell Biol.* 121:1083–1093.

Scheele, R. B., L. G. Bergen, and G. G. Borisy. 1982. Control of the structural fidelity of microtubules by initiation sites. *J. Mol. Biol.* 154:485–500.

Scholey, J., J. Heuser, J. Yang, and L. Goldstein. 1989. Identification of globular mechanochemical heads of kinesin. *Nature (Lond.)*. 338:355–357.

Song, Y.-H., and E. Mandelkow. 1993. Recombinant kinesin motor domain binds to β-tubulin and decorates microtubules with a B-surface lattice. *Proc. Natl. Acad. Sci. USA*. 90:1671–1675.

Steffen, W., and R. W. Linck. 1988. Evidence for tektins in centrioles and axonemal microtubules. *Proc. Natl. Acad. Sci. USA*. 85:2643–2647.

Svoboda, K., C. F. Schmidt, B. J. Schnapp, and S. M. Block. 1993. Direct observation of kinesin stepping by optical trapping interferometry. *Nature (Lond.)*. 365:721–727.

Vale, R. D., T. S. Reese, and M. P. Sheetz. 1985. Identification of a novel force-generating protein, kinesin, involved in microtubule-based motility. *Cell*. 42:39–50.

Wade, R. H., and D. Chretien. 1993. Cryoelectron microscopy of microtubules. *J. Struct. Biol.* 110:1–27.

Walker, R., and M. P. Sheetz. 1993. Cytoplasmic microtubule-associated motors. *Annu. Rev. Biochem.* 62:429–451.

Witman, G. B. 1992. Axonemal dyneins. *Curr. Opin. Cell Biol.* 4:74–79.

Yang, J., R. Laymon, and L. Goldstein. 1989. A three-domain structure of kinesin heavy chain revealed by DNA sequence and microtubule binding analyses. *Cell*. 56:879–889.